Engineering Notes

ENGINEERING NOTES are short manuscripts describing new developments or important results of a preliminary nature. These Notes cannot exceed 6 manuscript pages and 3 figures; a page of text may be substituted for a figure and vice versa. After informal review by the editors, they may be published within a few months of the date of receipt. Style requirements are the same as for regular contributions (see inside back cover).

Evaluation of Low Reynolds Number Turbulence Models for Attached and Separated Flows

A. Sugavanam*
Lockheed-Georgia Company, Marietta, Georgia

Introduction

TURBULENCE modeling still remains a major stumbling block in the computations of flow past complex aerodynamic shapes. While Reynolds stress models have enjoyed a reasonable success in free shear flows, the presence of walls poses formidable difficulties for these models in separated flows. Some of the advanced solution schemes for the time-averaged Navier-Stokes equations[1] presently use only the Baldwin-Lomax algebraic model.[2] Also, it has been found that the use of higher order turbulence models does not necessarily guarantee a better prediction capability in wall-bounded shear layers. However, several complex flows of significant practical importance (such as flow past a multielement or a circulation-controlled airfoil) cannot be meaningfully predicted without the use of higher order turbulence models. The use of simpler models in these problems requires estimating different length scales in different flow regions, and this task is almost as complex as solving the transport equations for simulating turbulence. The purpose of this Note is to examine the performance of some of the near-wall turbulence models using well-established mean flow solvers for attached and mildly separated flows.

Solution Procedure

The turbulence models considered in this Note are the modified Baldwin-Lomax algebraic model,[2] the Jones-Launder k-ϵ model,[3] the Chien k-ϵ model,[4] and the Wilcox-Rubesin k-ω^2 model.[5] The mean flow solvers chosen for the boundary-layer and time-averaged Navier-Stokes equations are Cebeci's, two-dimensional boundary-layer code[6] and the time-averaged full Navier-Stokes solver[7] developed at the Lockheed-Georgia Company. The turbulence model equations are solved along with the mean flow equations using the Alternating Direction Implicit (ADI) line procedure similar to the block procedure outlined for the mean flow solver described in Ref. 7. True wall boundary conditions are employed for these model equations instead of resorting to the wall function approaches. At the far field, the normal gradients of the turbulence field variables are set to zero. The details of the model equations and solution procedure can be found in Ref. 8.

Results and Discussion

For brevity, the results of the boundary-layer computations are not presented here, since they can be found elsewhere.[8] The primary conclusion from the boundary-layer study is that the Chien k-ϵ model is able to predict some of the details more accurately than other two-equation models considered. Further, it is found that the Chien k-ϵ model is relatively free of several numerical problems that occur in the vicinity of the wall. Thus, the time-averaged Navier-Stokes results are presented only with the Chien k-ϵ and Baldwin-Lomax models.[8]

The modified Baldwin-Lomax algebraic model presented some difficulties in estimating the outer-layer eddy viscosity. Recently, Visbal and Knight[9] pointed out certain discrepancies in calculating the length scale in the outer region in the neighborhood of a shock. In the present computations, with an impulsive start, similar discrepancies were noticed even in the absence of shock or separation. Figure 1 shows the distribution of the Baldwin-Lomax length-scale function, F across the lower-surface boundary layer near the trailing edge of an NACA 0012 airfoil at a Mach number of 0.8, Reynolds number of 2×10^6, and an angle of attack of 2 deg. F_{max} is seen to occur very close to the wall and, consequently, the length scale and eddy viscosity become very small. This figure also shows several local peaks of the function F and the corresponding eddy viscosities associated with these peaks. Thus, by choosing an appropriate peak that really belongs to the outer region, it is possible to eliminate inconsistent eddy viscosities. In the present computations, the search for F_{max} is confined to a region beyond $y^+ = 100$.

The time-averaged Navier-Stokes computations were performed for the cases of transonic flow past an RAE2822 airfoil and subsonic flow past an NACA 0012 airfoil.

Transonic flow past an RAE2822 airfoil is considered at a subcritical Mach number of 0.676, angle of attack of 1.93 deg, and a Reynolds number of 5.7×10^6 in an effort to simulate the measurements of Cook, et al.[10] (the experimental geometric angle of attack for this case is 2.4 deg.) A 149×60 C-grid was generated for this case with the first grid point immediately adjacent to the airfoil located at a distance of $y^+ = 0.7$ away from the surface. No transition is assumed, and the fully turbulent computations were initiated with an impulsive start, using the Baldwin-Lomax algebraic model with a variable time step. After 2000 iterations, the Chien k-ϵ model was introduced, and 2000 additional iterations were performed with constant time steps. By this time the L2 norm for the density had been reduced by four orders of magnitude and the lift coefficient had converged to four decimal places. Figure 2 shows the results of these computations for the surface pressure along with the experimental data. The agreement between the prediction and experiment is excellent, except at the leading edge. Table 1 gives the lift and drag predictions of the present computations along with the results of other prediction procedures. The lift coefficient predicted by the present method is in excellent agreement with the measurements. While the drag predictions are higher than the measurements, they are found to be in accord with other predictions.

Computations for the supercritical flow past the same airfoil are considered at a Mach number of 0.73, an angle of attack of 2.79 deg, and a Reynold number of 6.5×10^6. These computations are compared with the measurements at a geometric angle of attack of 3.19 deg. The computations with the Chien k-ϵ model show a mild separation at the foot of the shock. Figure 3 shows the predicted surface-pressure distribution for the case along with the measurements. The agreement

Presented as Paper 85-0375 at the AIAA 23rd Aerospace Sciences Meeting, Reno, NV, Jan. 14-17, 1985; received Jan. 16, 1985; revision received Aug. 22, 1985.

*Scientist, Associate. Member AIAA.

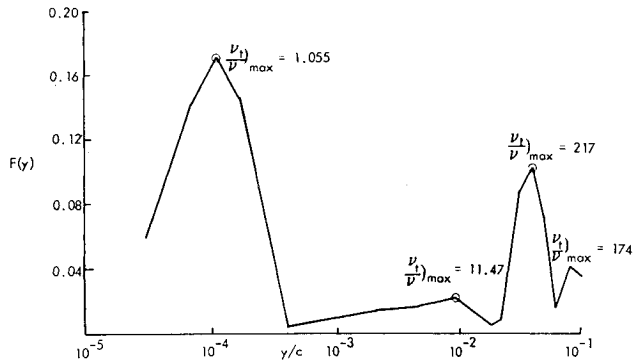

Fig. 1 The Baldwin-Lomax function across the boundary layer.

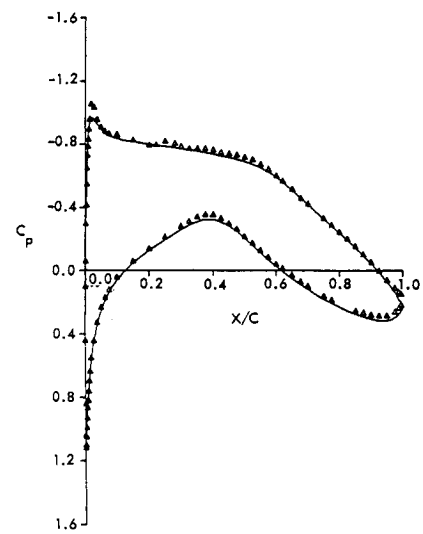

Fig. 2 Surface-pressure distribution of RAE 2822 airfoil at $Re = 5.7 \times 10^6$, $M_\infty = 0.676$ and $\alpha = 1.93$ deg (—present computation; Δ Cook, et al.[10] data).

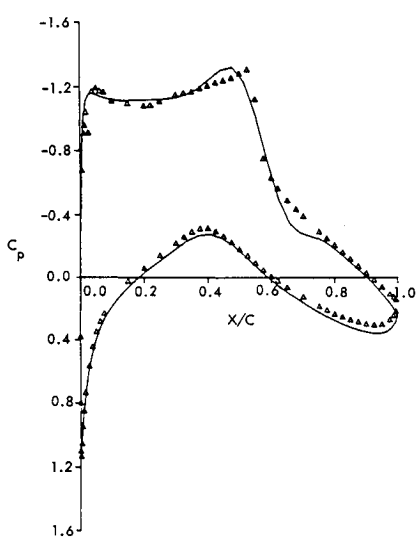

Fig. 3 Surface-pressure distribution of RAE 2822 airfoil at $Re = 6.5 \times 10^6$, $M_\infty = 0.73$ and $\alpha = 2.73$ deg (—present computation; Δ Cook, et al.[10] data).

is excellent, except in the vicinity of the shock. Table 2 shows the present lift and drag predictions for this case along with those from other prediction procedures. While the present load predictions are slightly higher than the measured values, they are comparable to Pulliam's[1] results. The local skin-friction predictions are 10-15% higher than the measured value. There is no significant difference between the turbulence models used in the estimation of skin friction.

Recently, Barton and Pulliam[13] performed both viscous and inviscid computations for subsonic flow past an NACA 0012 airfoil at a Mach number of 0.301 and at the very high angle of attack of 13.5 deg. They found that their inviscid computations predicted unrealistic unsteady oscillations, whereas their

Table 1 RAE2822 airfoil loads ($M_\infty = 0.676$, $Re = 5.7 \times 10^6$)

	α, deg	C_L	C_D
Experiment[10]	2.4	0.566	0.0085
Corrected experiment	1.93	0.566	0.0085
Mehta[11]	1.80	0.566	0.0094
Pulliam[1]	1.93	0.587	0.0102
Coakley[12]	2.4	0.620	0.0140
Present	1.93	0.569	0.0112

Table 2 RAE2822 airfoil loads ($M_\infty = 0.73$, $Re = 6.5 \times 10^6$)

	α, deg	C_L	C_D
Experiment[10]	3.19	0.803	0.0168
Corrected experiment	2.79	0.803	0.0168
Mehta[11]	2.79	0.793	0.0177
Pulliam[1]	2.79	0.825	0.0195
Coakley[12]	3.19	0.825	0.0240
Present	2.79	0.823	0.0201

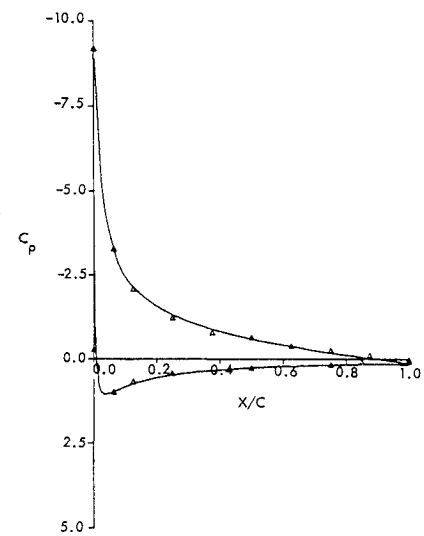

Fig. 4 Surface-pressure distribution of NACA 0012 airfoil at $Re = 3.91 \times 10^6$, $M_\infty = 0.301$, and $\alpha = 13.5$ deg (—present computations; Δ McCroskey, et al.[14] data).

viscous computations at a Reynolds number of 3.91×10^6 agreed very well with the measurements of McCroskey et al.[14] Since this forms an interesting test case for checking the predictive potential of time-averaged Navier-Stokes codes, the present procedure is applied to this case. A 151×50 C-grid was generated with the closest grid point adjacent to the airfoil located approximately a distance 0.00007 chord away from the airfoil, and the computational outer boundary located 6 chords away from the airfoil. The computations with the Baldwin-Lomax model were continued to 4000 iterations in order to detect any unsteadiness, if present. The converged steady-state results indicate a very small separated region near the trailing edge. Figure 4 shows that the computed and measured surface pressure distributions are in excellent agreement. There is a small supersonic region near the leading edge where the Mach number reaches $M = 1.22$. This also is consistent with the computations of Barton and Pulliam.[13]

Conclusions

For the airfoil cases considered herein, both the Baldwin-Lomax and Chien k-ϵ models perform very well in predicting the surface-pressure distribution and lift coefficient. However, it was noticed that some caution must be exercised when using the Baldwin-Lomax algebraic model in computing the length scale in the outer region in order to avoid spurious eddy-viscosity values. There was no improvement realized in predicting skin friction with the use of higher order models for the cases studied. The main advantage of the k-ϵ model over the algebraic models for complex turbulent flows existing at

this time appears to be the elimination of the arbitrary prescription of length scales, resulting in a more realistic estimation of the eddy viscosity in the wake.

References

[1]Pulliam, T. H., "Euler and Thin Layer Navier Stokes Codes: ARC2D, ARC3D," Notes for Computational Fluid Dynamics Users Workshop, The University of Tennessee Space Institute, Tullahoma, TN, March 1984.

[2]Baldwin, B. S. and Lomax, H., "Thin Layer Approximation and Algebraic Model for Separated Turbulent Flows," AIAA Paper 78-257, 1978.

[3]Jones, W. P. and Launder, B. E., "The Prediction of Laminarization with a Two-Equation Model of Turbulence," *International Journal of Heat and Mass Transfer,* Vol. 15, Feb. 1972, pp. 301-314.

[4]Chien, K. Y., "Predictions of Channel and Boundary Layer Flows with a Low Reynolds Number Turbulence Model," *AIAA Journal,* Vol. 20, Jan. 1982, pp. 33-38.

[5]Wilcox, D. C. and Rubesin, M. W., "Progress in Turbulence Modeling for Complex Flow Fields, Including Effects of Compressibility," NASA TN 1517, 1980.

[6]Bradshaw, P., Cebeci, T., and Whitelaw, J. H., *Engineering Calculation Methods for Turbulent Flow,* Academic Press, New York, 1981.

[7]Tassa, Y., "An Implicit Method for Solving the Navier-Stokes Equations with Applications to Shock-Boundary Layer Interactions," Lockheed-Georgia Co., Marietta, GA, Research Rept. LG79RR001, 1979.

[8]Sugavanam, A., "Evaluation of Low Reynolds Number Turbulence Models for Attached and Separated Flows," AIAA Paper 85-0375, Jan. 1985.

[9]Visbal, M. and Knight D., "The Baldwin-Lomax Turbulence Model for Two-Dimensional Shock-Wave/Boundary-Layer Interactions," *AIAA Journal,* Vol 22, July 1984, pp. 921-928.

[10]Cook, P. H., McDonald, M. A., and Firmin, M.C.P., "Aerofoil RAE2822—Pressure Distributions, and Boundary Layer and Wake Measurements," AGARD AR138, 1979.

[11]Mehta, U., "Reynolds-Averaged Navier-Stokes Computations of Transonic Flows Around Airfoils," Paper presented at the Second Symposium on Numerical and Physical Aspects of Aerodynamic Flows, Long Beach, CA, Jan. 1983.

[12]Coakley, T. J., "Turbulence Modeling Methods for the Compressible Navier-Stokes Equations," AIAA Paper 83-1593, July 1983.

[13]Barton, J. T. and Pulliam, T. H., "Airfoil Computation at High Angle of Attack, Inviscid and Viscous Phenomena," AIAA Paper 84-0524, Jan. 1984.

[14]McCroskey, W., McAlister, K., Carr, L., and Pucci, S., "An Experimental Study of Dynamic Stall on Advanced Airfoil Sections. Vol. 1, Summary of Experiment," NASA TM 84245, 1982.

A Simple Device for Wind Shear Measurement

H. Nelles* and R. W. Staufenbiel†
Aachen University of Technology
Aachen, Federal Republic of Germany

Introduction

WIND shear at low-level altitudes has been recognized as a potential safety problem to aircraft, especially during final approach and landing. Accidents of a DC-10 at Boston in December 1973 and a Boeing 727 at New York in June 1975, identified as wind shear accidents,[1,2] focused attention on this atmospheric phenomenon. Hazard may arise from the shear-induced change in horizontal wind velocity along the flight path or from the existence of a vertical wind component. In these conditions, a significant change in the wind velocity vector can result in a dangerous rate of descent.

Research activities are under way involving ground-based and airborne equipment to provide a pilot with suitable wind shear alert and energy management information. An airborne sensing system, if available, could also be used to gather meteorological data, especially wind vectors, and could be used to study their dependence on altitude and orographic conditions. These measurements could help to model the atmosphere in a more realistic way than at present, which is needed for realistic computer simulations.

Various physical effects can be used for sensing wind shear. Optical methods such as Laser Doppler Anemometers (LDA) and a combination of air and inertial data are the main candidates for airborne equipment.

This Note suggests a simple pneumatic sensing device that measures the difference of the dynamic pressures at two height positions on an airplane. This difference causes a mass flow through a pneumatic duct system. The velocity of this flow is measured by a special hot-wire probe.[3]

Experimental Approach

A single-engine light airplane, Socata Morane 893E, was used as the platform for the sensor system. A movable boom 2.3 m long was pivoted at the wing tip on the left-hand side and could be turned in a vertical position. The boom carried a pair of pitot tubes at each end connected by a hose. In case of a vertical shear flow the pitot tubes sense different total pressures which lead to a mass flow in the hose. The velocity of this mass flow is measured by a special hot-film probe (Westerboer type) operating in a constant-temperature mode and imbedded in the duct. The error due to varying air temperature is reduced by regulating the temperature before the flow passes the probe. The Morane carried an elaborate data acquistion system which additionally provided airspeed, altitude, and climb speed for determining shear flow and wind profiles. The flight data were recorded by an analog and a digitial recording system supported by an Apple II E microcomputer, which was also used for processing the data immediately after each flight. The testing of the sensor and the data acquisition system have been accomplished. The first application, planned in cooperation with meteorologists, is concerned with a field analysis of airplane approaches under strong wind shear conditions. In this program shear gradients and dynamical reactions of the disturbed airplane will be evaluated simultaneously.

Analysis Scheme

The total pressures at two different probe positions (locations 1 and 2) are given by

$$P_{t1} = P_{s1} + \tfrac{1}{2}\rho_1 (\vec{V}_{\mathrm{TAS}} + \delta\vec{U}_1)^2 \tag{1}$$

$$P_{t2} = P_{s2} + \tfrac{1}{2}\rho_2 (\vec{V}_{\mathrm{TAS}} + \delta\vec{U}_2)^2 \tag{2}$$

where the wind field vector U is partly included in the measurement of the true airspeed so that only the wind variation related to the position of the airspeed sensor has to be considered in δU_1 and δU_2. If the pitot probes are arranged at different height positions (distance Δh), the differences of the data between locations 1 and 2 may be written as

$$\frac{\Delta P_t}{\Delta h} = \frac{\Delta P_s}{\Delta h} + \tfrac{1}{2} V_{\mathrm{TAS}}^2 \frac{\Delta\rho}{\Delta h} + \rho \vec{V}_{\mathrm{TAS}} \frac{\Delta\vec{U}}{\Delta h} \tag{3}$$

where we have put $\rho = \tfrac{1}{2}(\rho_1 + \rho_2)$ and assumed that $\delta U \ll V_{\mathrm{TAS}}$. The difference in the static pressure is eliminated

Received April 3, 1985; revision received July 10, 1985.

*Research Engineer, Department of Aerospace Engineering.

†Professor of Aerospace Engineering, Department of Aerospace Engineering. Associate Fellow AIAA.